

One-Dimensional Calculation Including the Space Charge Effects of FEL Amplifiers

Tae Hun CHUNG and Jae Koo LEE¹

Department of Physics, Dong-A University, Pusan 604-714, Korea

¹*Department of Physics, Pohang Institute of Science and Technology,
Pohang 790-600, Korea*

(Received November 24, 1992)

Numerical calculations are performed based on the one-dimensional model for a tapered FEL amplifier with the combined helical wiggler and axial guide magnetic field operating in Raman regime. The longitudinal electric field due to space charge bunching can be formulated either by solving the coupled Maxwell and linear fluid equations or by solving the coupled kinetic and longitudinal wave equations. Both formulations are incorporated into the numerical code and the simulation results are compared. The criterion for the consideration of the space charge effect depends on the value of the electron beam parameter $\xi (\xi^2 = e^2 n_b / \gamma_0 m c^2 k_w^2)$. Besides, the perspective parameter studies are performed.

§1. Introduction

Many theoretical and experimental researches have been devoted to Free-electron laser (FEL) which generates stimulated emission of light by passing a relativistic electron beam through the spatially periodic field of a wiggler magnet.¹⁻³⁾ There are now many FEL experiments that have explored a wide range of physical parameters and system configurations. Several FEL experiments operate at moderately high beam current and make use of a magnetic guide field to steer the electron in the axial direction.⁴⁻⁶⁾

The electron trajectories are strongly modified by the presence of an axial guide field, particularly when the wiggler-induced helical motion is close to resonance with the cyclotron period in the axial magnetic field.⁷⁾ This gyroresonance strengthens the FEL interaction by increasing the amplitude of the helical motion. And the axial magnetic field directly affects the strength of the FEL coupling through its effect on the ponderomotive potential.^{8,9)}

Operating an FEL at high beam currents in the collective Raman regime achieves high powers and high efficiencies. For an FEL system employing very high beam currents, the term representing the effect of high space charge density should be retained in the equa-

tion of motion of the electron. In this regime, the entire electron beam takes part in the interaction, but collective effects are important only when the fluctuating space charge potential is comparable to the ponderomotive potential. The emission from a Raman FEL results from the interaction between the slow space charge wave on the electron beam and the electromagnetic mode.

An FEL can be operated either as an oscillator or as an amplifier. In an amplifier mode, the gain in a single traverse needs to be significant, and this requires an intense electron beam. In this configuration, the resonator mirrors are not used for optical feedback so that high gain in a single pass is desirable. The electron current is typically larger than in the oscillator case so that significant energy can be converted to radiation at the end of the undulator.

In this study, we develop a one dimensional simulation code for a tapered FEL amplifier with the combined helical wiggler and axial guide magnetic field operating in Raman regime. Using this code, we investigate the system characteristics with varying operating parameters. And we investigate the effect of the longitudinal electric field due to space charge on the output power and the extraction efficiency on the grounds that this space charge effect can not be ignored in high cur-

rent Raman regime. We present two different approaches of obtaining the approximate formula of the longitudinal electric field due to the space charge. Since we adopt a one-dimensional model, various practically interesting effects have been neglected. These effects include optical guiding, diffraction, transverse betatron motion, electron beam waist, effects of finite pulse width.

Similar self-consistent amplifier calculations have been carried out by Prosnitz *et al.*¹⁰ for a linearly polarized wiggler FEL in the Compton regime. The two-dimensional simulations of a high gain FEL amplifier have been performed by Fawley *et al.*¹¹ An extended one-dimensional approach has been undertaken by Wurtele *et al.*¹² They examined the influence of rf input power on the saturation and detuning characteristics of the laser, and examined that power as a function of the beam current and the wiggler field amplitude and length. The three-dimensional simulations have been undertaken by Freund and Ganguly,¹³ and by Tran and Wurtele.¹⁴

The physics of the collective FEL is well described by electron trapping in the potential formed by the combined action of the ponderomotive and self-consistent space-charge forces. Usually, the space charge field is expanded in a superposition of the Gould-Trivelpiece mode¹⁵ of the beam. The collective Raman interaction couples the TE and TM modes of a cylindrical and rectangular waveguide with each of the Gould-Trivelpiece modes having an azimuthal mode number of $l=0$.¹⁶

The motivation for the present work is to develop a simple theory and simulation code which can be utilized to investigate the overall characteristics of FEL performance without resorting to 3-D codes. We do not take accounts of the wave-guide mode, thus instead of Gould-Trivelpiece mode self-consistent electrostatic field is calculated for the space charge effect. In this work, firstly we incorporate the longitudinal electric field due to space charge bunching into the main formulation by employing the cold fluid description of the electron beam which proved to be appropriate for dealing with intense low energy electron beam. Secondly, we compare the result with the more

accurate formulation^{12,14} of the space charge effect which can be obtained solving the coupled kinetic and longitudinal wave equations.

The organization of this paper is as follows; In §2 we present our model and discuss how we account for the modification of the one-dimensional equation of motion for an electron by the space charge effect. In §3 we present the results of simulations and investigate the effect of the space charge on FEL performance, and discuss the details of the parameters study that are relevant to the specific FEL structure. Finally, we present our conclusions in §4.

§2. Simulation Model

In this system, a helical undulator field is superimposed to the axial guide field as

$$\mathbf{B} = B_w(\mathbf{e}_x \cos k_w z + \mathbf{e}_y \sin k_w z) + B_0 \mathbf{e}_z, \quad (1)$$

where $k_w = 2\pi/\lambda_w$ and λ_w is the period of the undulator.

The transverse components of velocity are written as^{1,9}

$$\begin{aligned} v_x &= \frac{\omega_{ce} k_w}{\gamma_0 \kappa^2} \cos k_w z \\ v_y &= \frac{\omega_{ce} k_w}{\gamma_0 \kappa^2} \sin k_w z, \end{aligned} \quad (2)$$

where

$$\kappa^2 = -k_w^2 + \frac{\Omega_{ce} k_w}{\gamma_0 v_{0z}} - \frac{\omega_{pe}^2}{\gamma_0 c^2},$$

ω_{ce} is the nonrelativistic electron cyclotron frequency in the helical field, Ω_{ce} is the nonrelativistic electron cyclotron frequency in the axial guide field, and $\omega_{pe}^2 = n_b e^2 / \epsilon_0 m$ is the nonrelativistic plasma frequency, and m is the electron rest mass.

The electromagnetic wave to be amplified is chosen to be left-hand circularly polarized and is given by

$$\begin{aligned} \mathbf{E}_l &= E_0(z)[\mathbf{e}_x \sin(k_s z - \omega t + \phi) \\ &+ \mathbf{e}_y \cos(k_s z - \omega t + \phi)]. \end{aligned} \quad (3)$$

The optical wave is traveling along the z -axis with wavelength $\lambda = 2\pi/k_s = 2\pi c/\omega$, the field strength E_0 , and the phase ϕ . From the rate equation at which the plane wave does work on the electron we obtain

$$\frac{d\gamma}{dz} = -\frac{eE_0K}{\gamma_0 mc^2} \sin \psi - \frac{eE_z}{mc^2}, \quad (4)$$

where $\psi = (k_s + k_w)z - \omega t + \phi(z)$ is the relative phase of the electron to the laser field, and the undulator parameter K is written as

$$K = \frac{\omega_{ce}}{ck_w(r-1-\xi^2)},$$

where $r = \Omega_{ce}/k_w v_{0z} \gamma_0$, $\xi^2 = e^2 n_b / \epsilon_0 m \gamma_0 c^2 k_w^2$. Note that r is the ratio of the wiggling period to the gyration period, and the electron beam parameter ξ denotes the relative measure of the space charge effects.

Usually we describe the system in terms of the inhomogeneous wave equation for the vector potential of the radiation field, the fluid equations for the density and velocity of the electron beam, and the Poisson equation for the self-consistent electrostatic potential of the space-charge wave. These equations form a closed set with which the system can be described self-consistently. From the linear fluid theory,⁹⁾ the amplitude of the electrostatic wave can be written in terms of the amplitude of the scattered electromagnetic wave as

$$E_z = -\frac{2E_0 \kappa^2 \gamma_0 \omega}{\omega_{ce}(k_s + k_w)} \epsilon_{em} \sin \psi, \quad (5)$$

where

$$\epsilon_{em} = \frac{k_s^2 c^2}{\omega^2} + \frac{\omega_{pe}^2}{\gamma_0 \omega^2} \frac{\omega - k_s v_{0z}}{\omega - k_s - \Omega_{ce}/\gamma_0} - 1,$$

is the electromagnetic dielectric function and the space charge wave is assumed to be synchronous with the ponderomotive wave, which can be justified in linear regime. Then eq. (4) is written as

$$\frac{d\gamma}{dz} = -\frac{k_s a_s K}{\gamma} (1 - \Phi) \sin \psi, \quad (6)$$

where

$$a_s = \frac{eE_0}{k_s m c^2}, \quad \Phi = \frac{2\gamma_0^2 \omega \epsilon_{em}}{(k_s + k_w) K^2 c}.$$

This approach takes the in-phase term of the principal mode of E_z among its Fourier series expansion.^{14,17)}

For Raman regime where the space charge wave is comparable to the ponderomotive wave, the term Φ must be retained in the equa-

tion of motion. We can write an equation for the rate of change of ψ as

$$\frac{d\psi}{dz} = \frac{d\phi}{dz} + k_w - k_s F, \quad (7)$$

where

$$F = \frac{1}{2\gamma^2} \left[1 + K^2 + \frac{a_s^2}{2} - \sqrt{2} K a_s \cos \psi \right].$$

Equations (6) and (7) yield a second-order equation for ψ

$$\begin{aligned} \frac{d^2 \psi}{dz^2} = & -\frac{K a_s k_s}{\gamma^2} \left[\frac{\sqrt{2}}{2} k_w \right. \\ & \left. + \frac{k_s}{\gamma^2} \left(1 + K^2 + \frac{a_s^2}{2} \right) \left(1 - \Phi - \frac{\sqrt{2}}{4} \right) \right] \\ & \times \sin \psi. \end{aligned} \quad (8)$$

Here we have assumed

$$\frac{d}{dz} \left(K^2 + \frac{a_s^2}{2} \right) = 0.$$

If we further assume γ is constant and equal to synchronous energy γ_r where

$$\gamma_r^2 = \frac{k_s}{2k_w} \left(1 + K^2 + \frac{a_s^2}{2} \right), \quad (9)$$

the usual pendulum equation is recovered;

$$\frac{d^2 \psi}{dz^2} = -\frac{2K a_s k_s k_w}{\gamma_r^2} (1 - \Phi) \sin \psi. \quad (10)$$

The synchrotron wave number in the presence of longitudinal space charge force is then given by

$$\Omega_{syn} = \left[\frac{2K a_s k_s k_w}{\gamma_r^2} (1 - \Phi) \right]^{1/2}. \quad (11)$$

It should be noted that eq. (11) is valid for the linear regime. According to the formalism of D. Prosnitz *et al.*,¹¹⁾ the resulting equations for the normalized wave amplitude and phase are

$$\frac{da_s}{dz} = \sqrt{2} K S \left\langle \frac{\sin \psi}{\gamma} \right\rangle, \quad (12)$$

$$\frac{d\phi}{dz} = \frac{\sqrt{2} K S}{a_s} \left\langle \frac{\cos \psi}{\gamma} \right\rangle - \left\langle \frac{1}{\gamma} \right\rangle, \quad (13)$$

where $S = \omega_{pe}^2 / 2k_s c^2$, the angular bracket $\langle \rangle$ denotes an ensemble average over the initial electrons.

The term E_z can also be obtained by solving

the longitudinal wave equation for the electrostatic field which results from the charge bunching in ψ space.^{12,14} An approximate solution is

$$E_z = \frac{2n_b e [\langle \sin \psi \rangle \cos \psi - \langle \cos \psi \rangle \sin \psi]}{\epsilon_0 (k_s + k_w)}. \quad (14)$$

Thus, eq. (4) can be written as

$$\frac{d\gamma}{dz} = -\frac{k_s a_s K}{\gamma} \sin \psi - a_z, \quad (15)$$

where

$$a_z = 4KS \frac{[\langle \sin \psi \rangle \cos \psi - \langle \cos \psi \rangle \sin \psi]}{(k_s + k_w)}.$$

We will compare the simulation results which takes into consideration of the space charge effect by implementing eq. (6) or eq. (15). Equations (6) (or (15)), (7), (12) and (13) now describe the one-dimensional motion of any electron in the specified field. Intergrating eq. (6) or eq. (15) by two step integration method,¹⁸ the energy of every electron with different phases can be calculated along the interaction region. The efficiency is defined as

$$\eta = \frac{\gamma_0 - \langle \gamma \rangle}{\gamma_0 - 1}. \quad (16)$$

It should be noted that the equations are derived by assuming a slow variation of the wave amplitude and phase and averaging over the fast oscillation.

§3. Simulation Results

(a) Study of operating parameters

Using the above equations (6) (or eq. (15)), (7), (12), (13) we calculate numerically the amplified wave amplitude throughout the interaction region and the nonlinear efficiency of the FEL system following the self-consistent evolution of the amplitude and phase of the wave. The propagation of radiation is described by the paraxial difference method on a spatial grid on axis with 500 grid points. About 400 test particles that are loaded with uniformly distributed phases move in γ , ψ space according to eqs. (6) and (7).

The code can design its own tapered wiggler; We have chosen to taper B_w with k_w held

Table I. Model parameters.

$B_0=12$ kG: axial guide field
$B_w=2$ kG: wiggler field
$\gamma=4.5$: relativistic factor
$J=10^7$ [A/m ²]: beam current density
$\lambda_w=3$ cm: wiggler period
$\lambda=5$ mm: radiation wavelength
$L=2.5$ m: interaction length
$E_0=1.5 \times 10^6$ [V/m]: input wave field
Taper: wiggler magnetic field is tapered as cosine function. Tapering percent is 90%, which represents the 10% of initial strength at the end of wiggler.

constant. Using the code, we perform the parameter study with respect to various operating variables. In this study, the peak wiggler magnetic field strength B_w in a period is from 2 kG to 5 kG, and the axial guide field strength B_0 is from 6 kG to 14 kG. We consider the variable wiggler magnetic field strength with tapering degree from 0 to 100%. The model parameters for single frequency simulation of the FEL is listed in Table I. The radiation wavelength is taken to be 5 mm. We assume that the beams are monoenergetic (no thermal spread), and are completely intermingled spatially.

It should be noted that there exists the possibilities of several different solutions of K and v_{0z} for a given set of the values of ω_{ce} , Ω_{ce} , k_w , γ_0 . The stable orbits are classified as the group-I ($r < 1$) and group-II ($r > 1$) orbits. Thus, the parameter study should be proceeded as; First, for a given values of ω_{ce} , Ω_{ce} , k_w , γ_0 , r -value should be determined by assessing v_{0z} from the stable orbit condition. Then K -value is determined automatically.

The output power gain is highest when the tapering degree is 90% under the sample parameters given in Table I. Figure 1 shows the output power gain as a function of the current density of the electron beam. It can be noted that the Raman effect actually reduces the gain relative to the prediction obtained without the inclusion of space charge effect, thus, for the dense beam case, the space charge effect should be considered. Above the current density level of 10^7 A/m², the saturation lengths are different for the both cases even though they result in comparable gain values. Figure 2 shows the variation of the out-

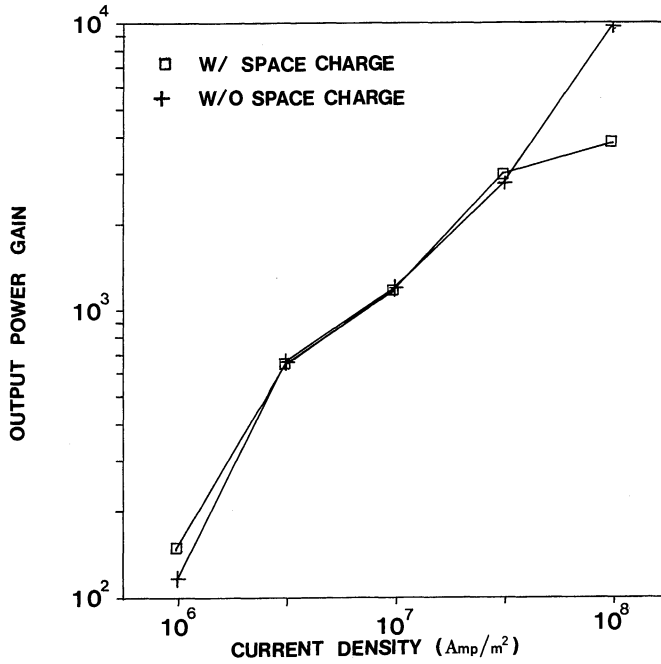


Fig. 1. Output power gain versus the current density of the electron beam. Rectangle shows the results with space charge effect, and cross symbol shows the result without the space charge effect.

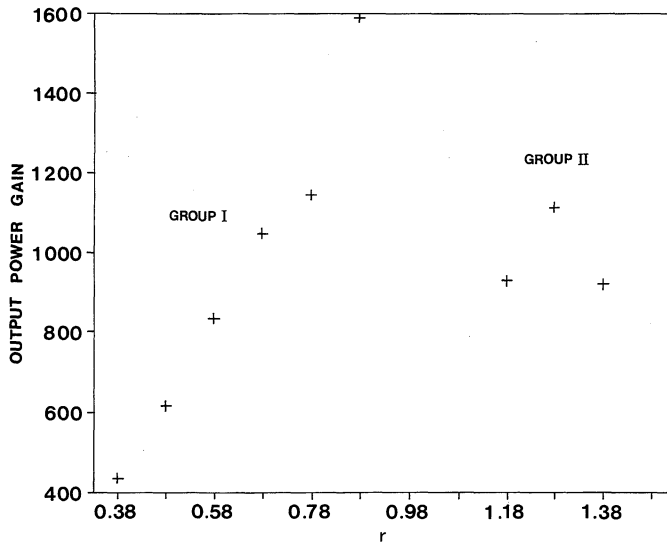


Fig. 2. Output power gain vs r -value varying the strength of the axial guide magnetic field.

put power gain with the r -value varying the strength of the axial guide field. It is shown that the output power gain increases with increasing axial guide field for $r < 1$ regime

(group-I orbits), and decreases again for $r > 1$ regime (group-II orbit). Near $r = 1$ (transition region), there is no power gain. For the sample parameters here, the optimal r -value is 0.88.

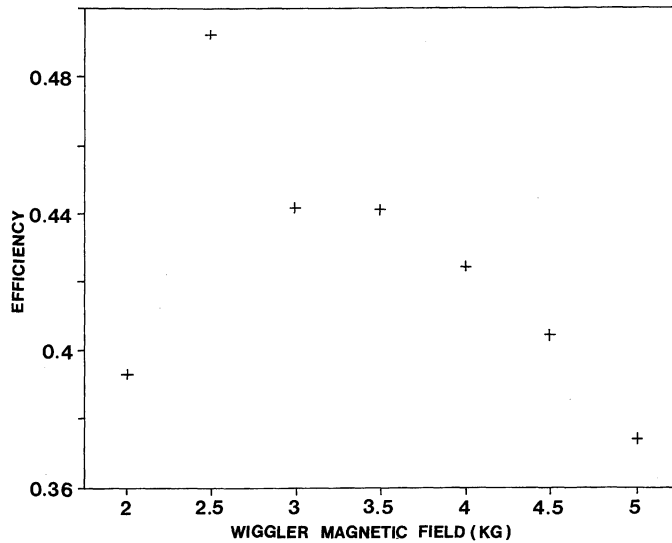


Fig. 3. The extraction efficiency versus the strength the wiggler magnetic field.

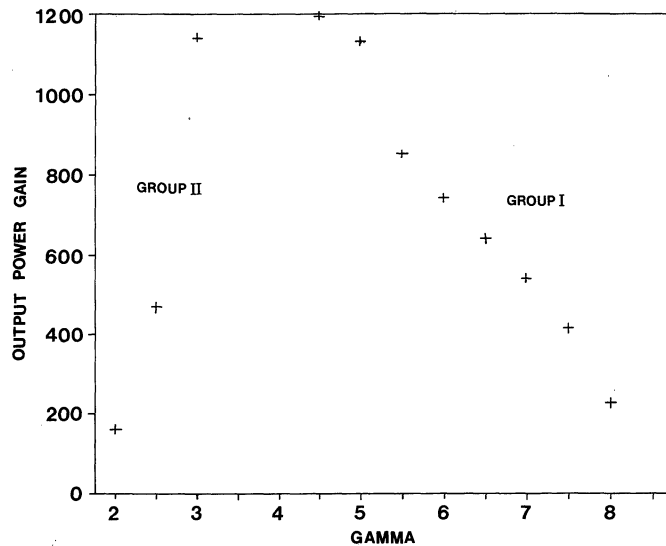


Fig. 4. The extraction efficiency as a function of relativistic factor of the electron beam.

The results are in accord with the previous studies.^{19,20} Figure 3 shows the relation between the efficiency and the strength of the wiggler magnetic field. In Fig. 3, the fact that the efficiency curve has maximum points reflects that there exists an optimal strength of the wiggler magnetic field to the specific condition. Under the model parameters considered here, the optimal strength is around 2.5 kG. Figure

4 represents the variation of the output power gain with the energy of the electron beam. As expected, the efficiency for the group-I orbits decreases monotonically with the beam energy. It is shown that there exists transition region (magneto-resonance) between group-I and group-II orbits where there is no power gain. Figure 5 shows the frequency dependence of the extraction efficiency for two value

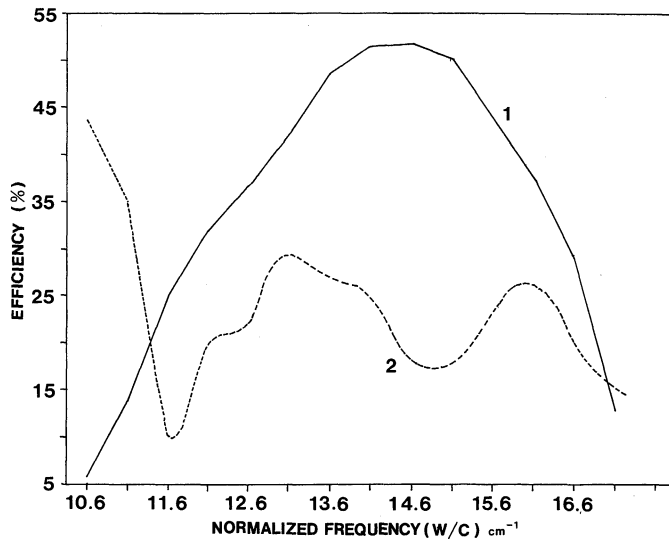


Fig. 5. Frequency dependence of the extraction efficiency: curve 1, $r=0.746$ (group-I); curve 2, $r=1.2$. (group-II).

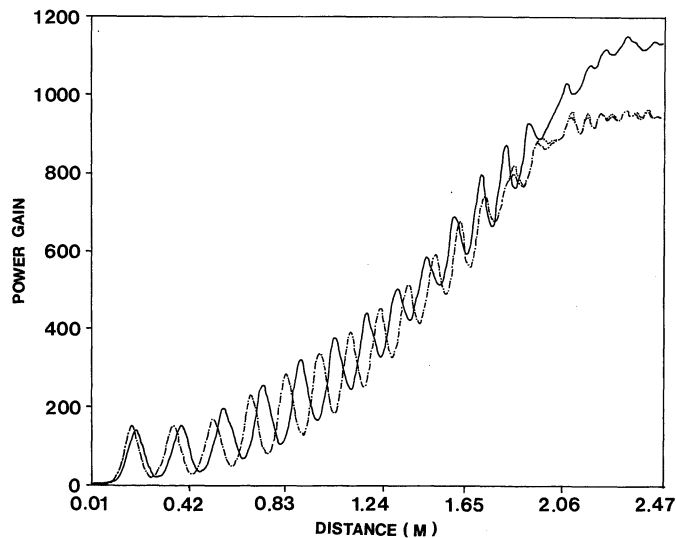


Fig. 6. The effect of longitudinal electric field due to space charge. Dashed line indicates the case not considering the effect, dotted line indicates the results implementing eq. (6), and solid line indicates the results implementing eq. (15). Here $B_w=2.5$ kG.

of $r=0.746$ (group-I) and $r=1.2$ (group-II). For group-I orbit, the FWHM is about 36%. The results are well in accord with analytic results.^{19,20)}

(b) *Space charge effect*

Next, the effect of the longitudinal electric field on the radiated laser power is manifested

in Figs. 6, 7, 8. When the sample parameters given in Table I are chosen, the space charge effect does not exhibit big differences. Especially in linear regime where the growth rate calculated from the linear dispersion relation yields the same results as those from the particle simulation, the models which incorporate

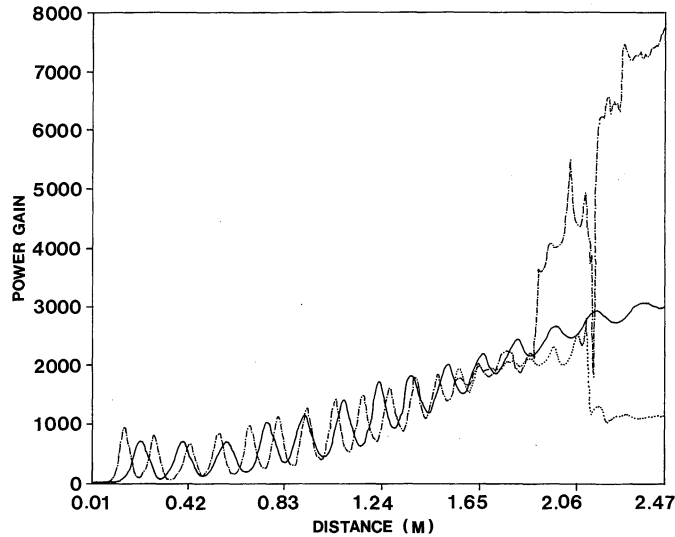


Fig. 7. The effect of longitudinal electric field due to space charge. Dashed line indicates the case not considering the effect, dotted line indicates the results implementing eq. (6), and solid line indicates the results implementing eq. (15). Here $J=5 \times 10^7$ [A/m²].

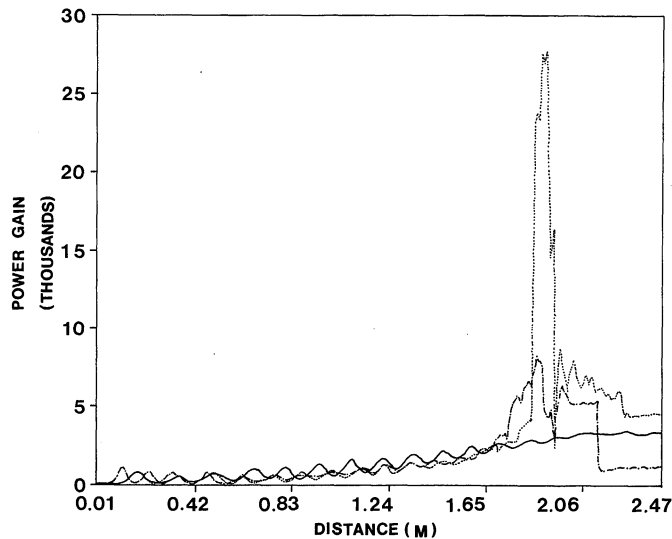


Fig. 8. The effect of longitudinal electric field due to space charge. Dashed line indicates the case not considering the effect, dotted line indicates the results implementing eq. (6), and solid line indicates the results implementing eq. (15). Here $J=5 \times 10^7$ [A/m²], $B_w=2.5$ kG.

eq. (6) and eq. (15) do not exhibit difference. And when the wiggler magnetic field is raised to 2.5 kG (with other parameters unchanged), the results of two cases are not different (Fig. 6). However, as the current becomes high, and the operating parameters approaches to the

magneto-resonance, the space charge effect plays a role of decreasing the radiation power by preventing the wave-particle resonance. In Fig. 7, the differences are manifested clearly. The model which does not consider the longitudinal electric field leads to unrealistic

spikes in power gain curve. But the models implementing the space charge effect yield more reliable results, especially the model implementing eq. (15) provides more reasonable evolution of the power gain along the distance than the implementation of eq. (6). In Fig. 8, where the wiggler magnetic field is raised to 2.5 kG, the model which does not account for the space charge effect yields the unrealistic spike in power gain curve. Just as the former case, the space charge model adopting eq. (6) gives the unreliable results which shows abrupt changes of power gain along the distance. The model employing eq. (15) provides the most accurate results. In eq. (6), we consider the longitudinal electric field due to space charge in phase with the ponderomotive wave. But, the out-of phase terms may be important for nonlinear evolution of the instability, and these two terms are incorporated into eq. (15). Thus, eq. (15) provides the accurate treatment of the space charge effect. Since eq. (6), which is derived from the linear fluid theory, can not treat the out-of phase terms, it can be stated that the results using eq. (6) only indicates the parameter regimes where the space charge effect play a significant role and the formulation can be used to obtain the synchrotron os-

cillation period in linear regime. From the Fig. 7 and Fig. 8 (where $\xi^2=0.19$), we can conclude that, for a FEL amplifier operating in Raman regime, the space charge effect should be considered to describe the system accurately. The criterion for the consideration of the space charge may be stated as; $\xi^2 > 0.15$.

It is noted that the presence of a strong axial magnetic field results in a markedly different behavior. Negative masslike effect occurs in which the electrons are accelerated as they lose energy to the wave. As a consequence, the electrons must be decelerated in order to maintain the wave-particle resonance. This is accomplished for group-II orbit by an upward taper in the wiggler field.²¹⁾ Figure 9 indicates this phenomenon clearly.

§4. Conclusion

In this paper we have developed a one-dimensional nonlinear theory and numerical simulation of the FEL amplifier with the tapered wiggler and the axial guide magnetic field. The FEL equations are analyzed numerically including the self-consistent evolution of the wave amplitude and phase. We then discuss the results from a series of simulation runs centered at the model operating

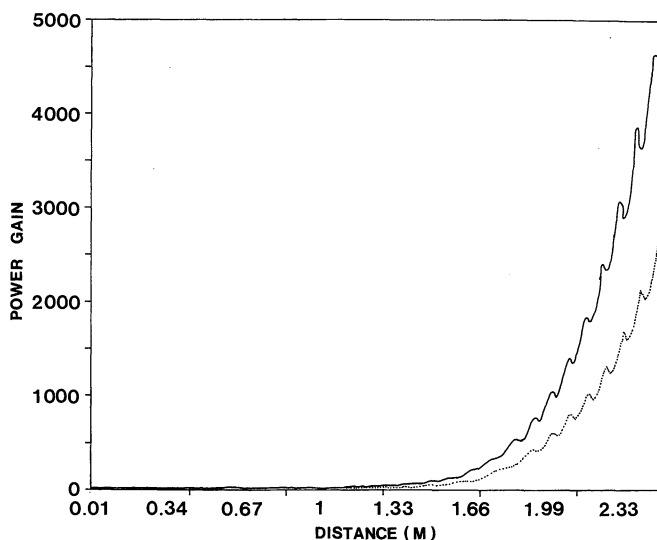


Fig. 9. Power gain in the amplifier along the interaction distance for parameters of sample cases; solid line with $r=1.15$ and $\omega/c=13.1 \text{ cm}^{-1}$, dashed line with $r=1.15$ and $\omega/c=12.1 \text{ cm}^{-1}$; 50% upward taper for both cases.

parameters. The conclusions are summarized as follows; (1) The space charge effect is important for the analysis of the Raman FEL. From a series of simulation runs we notice that the criterion for the consideration of the space charge effect depends on the value of the electron beam parameter ($\xi^2 = e^2 n_b / \epsilon_0 m \gamma_0 c^2 k_w^2$), and can be stated as $\xi^2 > 0.15$. The longitudinal electric field due to space charge can be well described by eq. (15). (2) The wavelength of radiation is shifted to longer values by the effect of the space charge oscillation. This can be seen from the expression of K , in which larger ξ produces larger K , thus increasing the wavelength of the em wave (This is sometimes called the d.c. effect of space charge). (3) The axial guide magnetic field is also found to have a profound effect on the nature of the efficiency enhancement process, for instance, the upward tapering for group-II orbits results in the efficiency enhancement. This parameter study can be used for the design and operation of Raman FEL amplifier.

References

- 1) T. Kwan and J. M. Dawson: Phys. Fluids **22** (1979) 1089.
- 2) N. M. Kroll, P. L. Morton, and M. N. Rosenbluth: IEEE J. Quant. Electron. QE-17 No. 8 (1981) 1436.
- 3) T. C. Marshall: *Free-Electron Lasers* (Macmillan, New York, 1985); C. Brau: *Free-Electron Lasers* (Academic Press, San Diego, 1990); P. Luchini and H. Motz: *Undulators and Free-Electron Lasers* (Oxford University Press, New York, 1990).
- 4) R. K. Parker *et al.*: Phys. Rev. Lett. **48** (1982) 238; J. Fajans, G. Bekefi, Y. Z. Yin and B. Lax: Phys. Fluids **28** (1985) 1995.
- 5) F. G. Yee and T. C. Marshall: IEEE Trans. Plasma Sci. PS-13 (1985) 480.
- 6) F. G. Yee, J. Masud, T. C. Marshall: and S. P. Schlesinger: Nucl. Instrum. & Methods Phys. Res. A **259** (1987) 104.
- 7) J. A. Pasour: Proc. SPIE **783** (1987) 55.
- 8) H. P. Freund and S. H. Gold: Phys. Rev. Lett. **52** (1984) 926.
- 9) T. H. Chung: J. Korean Phys. Soc. **21**, No. 3 (1988) 322.
- 10) D. Prosnitz, A. Szoke, and V. K. Neil: Phys. Rev. A **24** (1981) 1436.
- 11) W. M. Fawley, D. Prosnitz, and E. T. Scharlemann: Phys. Rev. A **30** (1984) 2472.
- 12) J. S. Wurtele, R. Chu, and J. Fajans: Phys. Fluids B **2** (1990) 1626.
- 13) H. P. Freund: Phys. Rev. A **37** (1988) 3371; H. P. Freund and A. K. Ganguly: IEEE Trans. Plasma Sci. **20** (1992) 245.
- 14) T. M. Tran and J. S. Wurtele: Comput. Phys. Commun. **54** (1989) 263.
- 15) N. A. Krall and A. W. Trivelpiece: *Principles of Plasma Physics* (McGraw-Hill, New York, 1973) p. 202.
- 16) A. K. Ganguly and H. P. Freund: Phys. Fluids **31** (1988) 387.
- 17) T. J. Orzechowski *et al.*: J. Quant. Electron. **21** (1985) 831.
- 18) S. Yakowitz and F. Szidarorszky: *An Introduction to Numerical Computation* (Macmillan Publishing Co., 1986) p. 305.
- 19) L. Friedland and A. Fruchtman: Phys. Rev. A **25** (1982) 2693.
- 20) L. Friedland and I. B. Bernstein: Phys. Rev. A **26** (1982) 2778.
- 21) H. P. Freund and A. K. Ganguly: Phys. Rev. A **33** (1986) 1060.